

Draft SPOTS Standard Part III (2)



CALIBRATION AND ASSESSMENT OF OPTICAL STRAIN MEASUREMENTS

Good Practice Guide to Grating (Moiré) Interferometry for In-plane Displacement/Strain Analysis

December 2005



1. Scope

Grating Interferometry with conjugate wavefronts (GI) is a technique of experimental full field and non-contact in-plane displacement measurement and strain analysis. It is also known under the name Moire Interferometry.

GI employs coherent laser illumination on the specimen with a reference high frequency grating and monitors the change of intensity pattern with a CDD camera. It provides full-field information about in-plane displacement vectors (in x and y directions) when the specimen is illuminated from different directions. The displacement fields are numerically differentiated in order to obtain strain maps. From the physical point of view, Grating Interferometry is based on monochromatic laser light illumination, use of a CCD camera, the superposition of two coherent beams diffracted at the specimen onto the CCD, and the change of the optical phase between the two beams due to displacements.

2. Reference materials

ISO Norms

ISO/TAG4/WG3, “Guide to the Expression of Uncertainty in Measurements (GUM), 1995, identical with EN130005: 1999: “Guide to expression of Uncertainty in Measurement”

ISO IEC 17025:1999: “General requirements for the competence of testing and calibration laboratories”

ISO 11145:2001 “Optical instruments – Lasers and laser-related equipment – Vocabulary and symbols”

ISO 10012:2003: “Measurement Management Systems- requirements for measurement processes and measuring equipment”

ASTM Standards

E 2208-02 Standard Guide for Evaluating Non-Contacting Optical Strain Measurement System

Other

VDI/VDE 2634 - Practical acceptance & verification methods for the evaluation of accuracy



3. Symbols and abbreviations

Symbol	Definition	Units
$a(x,y)$	local values of background intensity in an interferogram,	W/m^2
$b(x,y)$	local values of interferogram modulation function,	W/m^2
d_x, d_y	standard linear distance,	m
E^A, E^B	complex amplitudes of illuminating beam,	$\sqrt{(W/m^2)}$
E^A_{+1}, E^B_{-1}	complex amplitudes of +1 and -1 order beams diffracted at specimen grating,	$\sqrt{(W/m^2)}$
f	spatial frequency of the specimen grating,	1/mm
f_{ox}, f_{oy}	spatial frequencies of the linear carrier fringes added in the x or y ,	1/mm
k_x, k_y	actual number of pixels for standard linear distance,	-
$I_i(x,y)$	intensity values captured for i -th frame (interferogram with phase shift φ_i),	W/m^2
M	an integer	-
$N(x,y)$	actual integer number of the fringe,	-
p	pitch (distance between lines) of the grid,	m
n	half the number of pixels over which differentiation is performed	-
u, v	displacements (in- plane) in directions x and y	m
$w(x,y)$	displacement (out-of-plane) in direction z , due to the deformation of the specimen surface under load,	m
β	imaging system magnification,	-
δ_i	phase shift between sampling frames/points	rad
$\varepsilon_x, \varepsilon_y, \gamma_{xy}$	strain components referred to x - y rectangular coordinates,	m/m, %, μS
$\phi(x,y)$	phase of interferogram which is proportional to the quantity measured ,	rad
φ	phase shift between frames or sampling points	rad
λ	wavelength of light,	m
$+\theta, -\theta$	angle of the illuminating beams,	rad

Abbreviations

CCD	Couple Charge Device (camera with CCD detector)
CMOS	Complementary Metal-Oxide Semiconductor (camera with CMOS detector)
FEM	Finite Element Method
FT (FFT)	Fourier Transform (Fast Fourier Transform)
GI	Grating Interferometry
MEMS	Micro-Electro-Mechanical System
MOEMS	Micro-Opto-Electro-Mechanical System
RMS	Root Mean Square
SCPS	Spatial Carrier Phase Shifting
TPS	Temporal Phase Shifting



4. Terminology

<i>interferogram-</i>	fringe pattern with cosinusoidal modulation of its intensity formed by two coherent beams interference process.
<i>interferogram analysis-</i>	techniques for conversion of the intensity distribution at an output of a device producing an interferogram or a similar sinusoidal intensity fluctuation in space, into a continuous phase map representing the unambiguous difference of phase between the two interfering beams at any point at the output space.
<i>spatial frequency-</i>	one over the period (distance) of the amplitude variation appearing in the structure or its image ($f=1/d$).
<i>specimen grating-</i>	diffraction, high frequency linear grating (usually with $f>500$ lines/mm) attached to the specimen in such a way that specimen's in-plane displacements are transferred to the grating without errors.

5. Principles of the method

5.1 Introduction

Grating interferometry with conjugated wavefronts (GI) or the moiré interferometry method (both names are used in literature ^{1,2}) is a technique of experimental in-plane displacement measurement and strain analysis. GI employs a high frequency linear grating attached to a plane specimen subjected to load and in this sense it is similar to geometric moiré ^{3,4} with significantly enhanced sensitivity. It provides full-field information about in-plane displacement in the direction perpendicular to the grating lines. This displacement field is numerically differentiated in order to obtain strain maps. From a physical point of view grating interferometry is based on two phenomena:

- diffraction of coherent waves which incident symmetrically from two directions on the specimen grating to encode information about grating deformation caused by load,
- interference of those wave fronts, to visualize grating deformation in the form of an interferogram.

Grating interferometry can be applied in a purely qualitative manner by monitoring interferograms which represent lines of constant in-plane displacement. However nowadays GI is most often used in its digital version, which employs methods based on phase analysis of interferograms to determine digitally full-field displacement maps, followed by calculation of the strain map ⁵.

5.2 Basic principles

When a body is subjected to loads, strains produce deformations. In a arbitrary system of coordinates x, y , the basic components of displacement of a point in directions x and y are usually designated u and v , respectively. Also, the elongation (strain) changes with the distance between points on the body. The strains are related to displacements by well-known formulae of stress analysis (see also Figure 1):



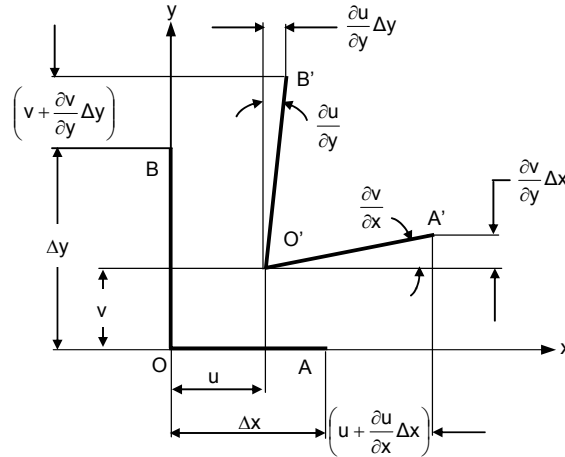


Fig.1. Relations between displacements and strains

$$\varepsilon_x = \frac{\partial u}{\partial x}, \quad \varepsilon_y = \frac{\partial v}{\partial y}, \quad \gamma_{xy} = \frac{\partial u}{\partial x} + \frac{\partial v}{\partial y} \quad (1)$$

$\varepsilon_x, \varepsilon_y, \gamma_{xy}$ strain components referred to x - y rectangular coordinates,
 $u(x,y), v(x,y)$ displacement in directions x and y , respectively,

Grating (moiré) interferometry is an experimental method used to determine the components of displacement (u, v) or strain ($\varepsilon_x, \varepsilon_y$). On a part subjected to analysis, a high frequency grating of equidistant lines is deposited by one of the methods described later. When the part is subjected to stresses, deformation of the part, and consequently of the grating applied to it, occurs. The deformed grating is then symmetrically illuminated by two mutually coherent beams with plane wave fronts (see Fig. 2). The incident angles of these beams are tuned to the first and negative first order diffraction angle of the specimen grating SG. In such a configuration +1 diffraction order of E_A and the -1 diffraction order of E_B propagate co-axially along the grating normal. The wave fronts of these beams are now not plane due to the deformation of the specimen grating and their complex amplitudes can be described as:

$$E_{+1}^A(x,y) \cong \exp\left\{i\left[\frac{2\pi}{p}u(x,y) + \frac{2\pi}{\lambda}w(x,y)\right]\right\} \quad (2)$$

$$E_{-1}^B(x,y) \cong \exp\left\{-i\left[\frac{2\pi}{p}u(x,y) - \frac{2\pi}{\lambda}w(x,y)\right]\right\} \quad (3)$$

Where: p is pitch (distance between lines) of the grid, E_{+1}^A, E_{-1}^B are complex amplitudes of +1 and -1 order beams diffracted at the specimen grating, $w(x,y)$ is the out-of-plane displacement function corresponding to the deformation of the specimen surface under load.

For simplicity, the amplitude of the diffraction orders has been normalized to unity.



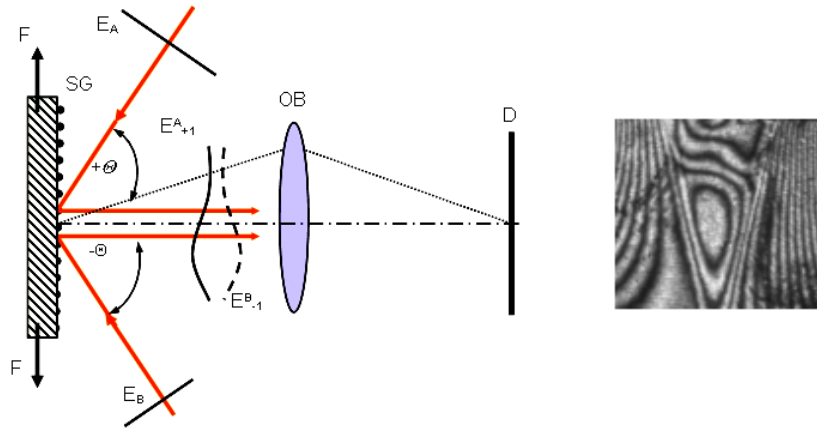


Fig. 2. Schematic representation of grating interferometry for in-plane displacement/strain studies. SG – specimen grating; OB – imaging optics; D – detector plane; E^A , E^B are complex amplitudes of illuminating beam, E_{+1}^A , E_{-1}^B – wavefronts of +1 and -1 diffraction order beams.

The wave front deformations caused by in-plane displacements are equal for both diffraction orders but longitudinally reversed. The wave front deformations due to out-of-plane displacements have the same value and sign in both interfering beams. Therefore the influence of out-of-plane displacements is eliminated by the interference. Thus assuming those out-of-plane displacements give only small variations in slope of the wave fronts⁶, the intensity distribution of the interferogram becomes

$$I(x,y) = |E_{+1}^A + E_{-1}^B|^2 = a(x,y) + b(x,y) \cos \left[\frac{4\pi}{p} u(x,y) \right] \quad (4)$$

where: $a(x,y)$ and $b(x,y)$ are the local values of background and contrast in the interferogram.

Note that the interference fringe represents a *line of constant displacement* u i.e. along a fringe $u = \text{constant}$, and the difference in the u value between two consecutive fringes is $\Delta u = p/2$. For example, when using a specimen grating of spatial frequency 1200 lines/mm the basic sensitivity is $0.47 \mu\text{m}$ per fringe order.

When the double beam illumination system is angularly misaligned, carrier fringes are introduced into the interferogram. The frequency of these fringes depends on the angle between interfering beams and on the wavelength of the light. This interferogram modification is utilized in automatic fringe pattern analysis methods which are described in section 10.

To obtain complete the strain information, a cross-line specimen grating is commonly used. A cross-line grating requires two pairs of illuminating beams for its readout as shown in Fig. 3. This configuration provides interferograms representing u -displacement (while A1+A2 are illuminating) and v -displacement (while B1+B2 are illuminating).

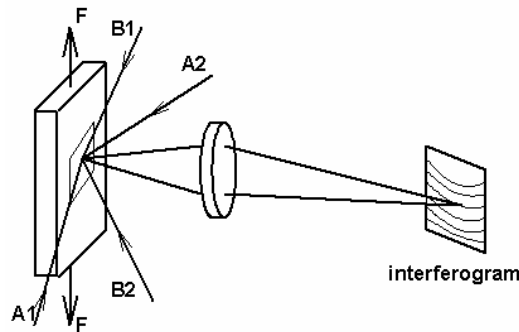


Fig. 3. A schematic diagram for a four-beam GI for capture of $u(x,y)$ and $v(x,y)$ interferograms.

The spatial frequency of the specimen gratings used in grating (moiré) interferometry depends on the incident angle θ and wavelength λ of the illuminating beams. The relation between these values is given as:

$$f = \frac{1}{p} = \frac{\sin\theta}{\lambda} \quad (5)$$

where f is the spatial frequency of the specimen grating.

From physical reasoning the theoretical upper limit for the specimen grating frequency is defined by $\theta = 90^\circ$. The lower limit depends on the mechanical system configuration. The angle θ cannot be too small because the illuminating and diffracted beams will have similar paths, and recording of an interferogram would be difficult. In practice, grating interferometers are designed for an angle θ higher than 20° . So, for an angle of $20^\circ < \theta < 90^\circ$ and visible light (from $\lambda=0.36 \mu\text{m}$ to $\lambda=0.78 \mu\text{m}$) the useful range of the spatial frequencies of specimen gratings is:

for $\lambda=0.36 \mu\text{m}$ $950 < f_{0.36} < 2800$ [lines/mm]

for $\lambda=0.78 \mu\text{m}$ $440 < f_{0.78} < 1300$ [lines/mm].

The standard specimen grating frequency (used most often in commercial and research systems) is 1200 lines/mm.

6. Apparatus

Grating interferometers consist of the following elements described from the light source to the sensor.

The light source: various types of lasers, e.g. gas or semiconductor diode lasers, are used. The required laser power depends primarily on the diffraction efficiency of the specimen grating, the magnification of the imaging system and the sensitivity of the CCD detector. The required coherence length of the laser radiation depends on the configuration of the interferometer beam-dividing head and the field of view but usually should not be lower than a few centimetres.

The beam-forming optical system. It transforms the laser beam into the illuminating beam with an appropriate diameter, a plane wave front and a homogenous intensity distribution. The quality of the collimating lenses or mirrors should be high enough to produce wave fronts that are plane to within a fraction of a wavelength.



The beam-dividing head. It enables symmetrical illumination of the specimen grating by one or two pairs of beams. The most popular interferometer heads are shown in figure 4. In the Lloyd configuration, a plane mirror M is placed perpendicularly to the specimen surface (Fig. 4a). Then half of the illuminating beam impinges directly on the specimen surface while the other half impinges indirectly in a symmetrical direction after reflection from a plane mirror. This is a simple set-up, which may be used for testing relatively big elements, however the use of one pair of illuminating beams implies that only a single in-plane displacement map is obtained. This configuration may be modified by adding a pair of mirrors M2 and M3 to obtain two mutually perpendicular components of in-plane displacements, as shown in Fig. 4b. In this three mirror interferometer head, two pairs of illuminating beams (selected from one source beam) are used to determine: $u(x,y)$ from A1+A2, and $v(x,y)$ from B1+B2.

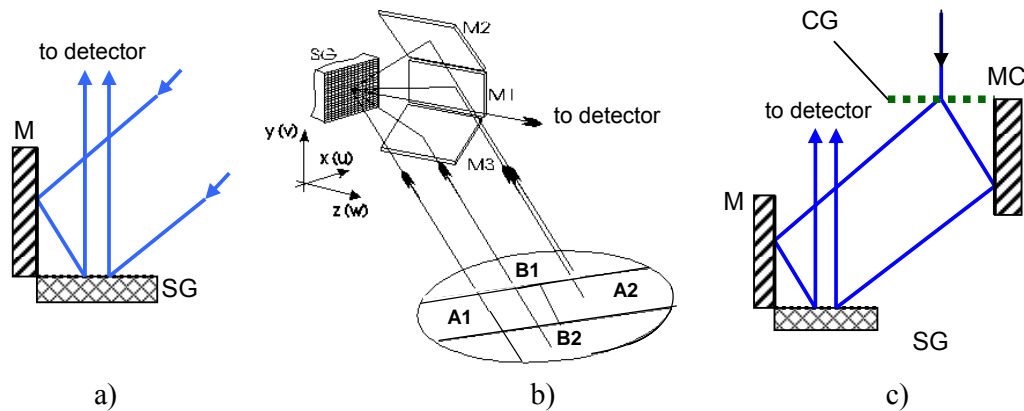


Fig. 4. Schematic diagrams of beam dividing interferometer heads.

a) Lloyd configuration; b) three mirror configuration; c) configuration with a compensation grating; M, M1, M2, M3 – mirrors; MC – compensating mirror; CG – compensation grating; SG – specimen grating.

Both heads described above are relatively simple but they are very sensitive to vibrations. Therefore in an unstable measurement environment it is advised to use Czarnek's configuration¹¹ (Fig. 4c), which is relatively insensitive to vibration. The illuminating beam is divided into two diffracted beams by compensating grating CG. Then these beams are directed onto the specimen grating by two mirrors M and MC. If the specimen and compensating gratings have the same frequencies, the influence of tilt of the illumination beams introduced by vibrations can be neglected. Additionally, this system is relatively insensitive to changes in the wavelength, so that a low temporal coherence laser can be used as the light source.

Interferogram modification devices serve to adapt the beams to the requirements of the interferogram analysis method being applied. The appropriate fringe frequency, required by the SCPS method, can be introduced by a tilting of the mirrors of the beam-dividing head and no additional element is needed in the system unless automatic adjustment is required. If the temporal phase shifting method is used, the appropriate phase shift has to be introduced into one of the specimen illuminating beams. This can be achieved by a variety of techniques including: a tilting parallel plate, grating shifting in the direction perpendicular to the grating lines, and rotation of a polarizer.

The specimen of interest with a high-frequency diffraction grating attached to its surface. It is necessary that the region under test has a plane and relatively smooth surface. The sample grating technology is described in section 7.



The imaging optics. The main role of this system is to image interferograms onto the CCD camera detector which is optically coupled with specimen plane. To decrease the distortion of the image, a non-focal optical system should be used.

A CCD or CMOS camera. A camera is used to sample the image with typical resolution of 256x256 or 512 x 512 points.

A schematic of a typical laboratory system with a three-mirror head is shown in Fig. 5. Light from the He-Ne laser is collimated by the optical system PS-CO. Next the beam after reflecting from the directional mirror M illuminates the mirrors of the interferometer head. After reflecting from the head mirrors, two pairs of beams are formed and they illuminate symmetrically the specimen with a cross-type reflected grating. A single pair of beams is selected by inserting one of the slot filters (F_x or F_y) into the path of the illuminating beam.

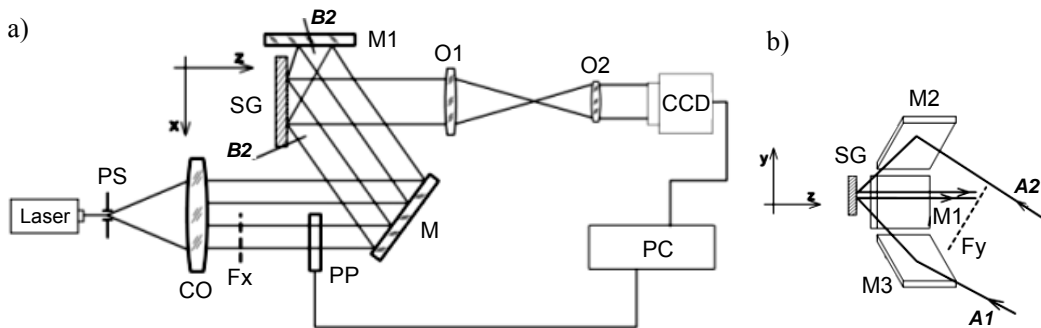


Fig. 5. Opto-mechanical configuration of laboratory grating interferometer: a) general scheme of system, b) 3D view at interferometric head.

PS – pinhole system, CO – collimating objective, F_x and F_y – slot filters, M1, M2, M3, M – mirrors, SG – specimen gratings, PP – tilted parallel plate, O1, O2 – imaging optics.

The interferograms are formed by interference of A1 and A2 beams or B1 and B2 beams after their diffraction at the specimen grating. The interferogram is imaged at the CCD detector which is optically coupled with the specimen plane by a non-focal optical system. The CCD is connected to a PC computer through a frame grabber. To facilitate the automatic computer-aided analysis, the temporal phase shifting technique is implemented by a tilting parallel plate PP (Fig. 5). The plate PP is inserted either into the beam A2 (for v measurements) or into the beam B2 (for u measurements). The angle of the plate can be adjusted using a stepper motor controlled by a computer. The temporal phase shifting method, TPS, requires stable conditions of measurement, during the capture of at least three phase-shifted interferograms. If this requirement cannot be fulfilled, the GI system should be modified for the spatial carrier phase shifting method (SCPS). The SCPS method requires the introduction into the interferogram of a controlled number of carrier fringes (section 10). This is achieved by tilting either the mirror M1 (for u) or mirror M2 and M3 (for v).

7. Sample preparation

Grating (moiré) interferometry requires the application on a specimen of a high frequency reflective phase-type grating. Such gratings are based usually on periodical variation of the surface relief, which is produced by a moulding process or through direct exposure of the element covered with photosensitive emulsion. The mould is usually a holographic plate with linear or cross-line grating produced by interference of two plane beams. Moulds with typical frequencies (600, 800,



1000, 1200 1/mm) are available commercially. A typical moulding process is shown in Fig. 6. A pool of liquid adhesive is poured onto the specimen and squeezed into a thin film by pressing against the mould. Epoxy adhesives are suitable. After hardening, the mould is prised off, leaving a reflective diffraction grating bonded to the surface of the specimen. The weakest interface in the system occurs between the gelatine of the photographic plate and the evaporated aluminium or gold, which accounts for the transfer of the film onto the specimen. The result is a reflective, high frequency, phase-type diffraction grating formed on the specimen. Its thickness is about 0.025 mm and the most popular frequency is 1200 1/mm. The master grid, from which the moulds are produced, generally originates for patterns produced by two-beam interference, which are recorded on holographic plates or in a photoresist. Sometimes the master grid is used to produce a submaster in silicone rubber and this submaster is used to replicate the phase grating in epoxy on the specimen surface, as explained above, but not using Al or Au layer in between. In this moulding process the surface finish is not particularly important - apart from cleanliness - since the curing materials fill the surface imperfections.

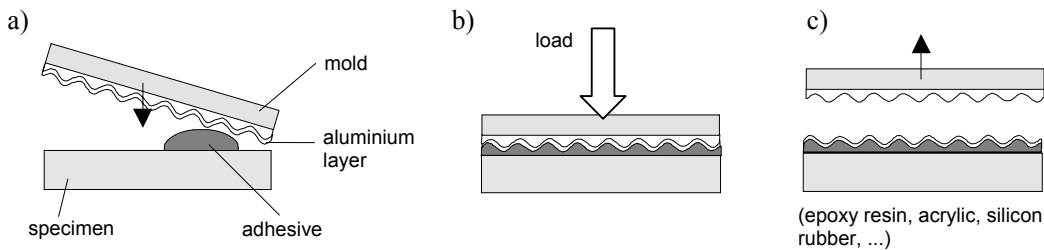


Fig. 6. Steps in producing the specimen grating by casting or replication process a) gluing, b) hardening, c) mould removing.

Sometimes the specimen grating produced by the replication process is considered too thick. This occurs especially in experiments performed on very small elements, which require special grating technology (so called “zero” thickness grating). Usually such a grating is produced in photoresist. A thin ($\sim 1 \mu\text{m}$) photoresist layer is spun onto the specimen and then exposed with two interfering laser beams (Fig. 7). If a simple, reflective grating is required (e.g. for material or fracture mechanics studies), the photoresist is developed and the relief is covered (by evaporation) with a thin aluminium or gold layer. If a grating is needed that is totally integrated (with for example a silicon element for MEMS, MOEMS studies), the development stage is followed by an etching procedure and the grating is produced directly in the material of the specimen. All zero-thickness gratings require surface finish of optical quality. Recently, special grating preparation techniques have been proposed including writing gratings directly onto the specimen surface by means of a high power laser or electron beam.

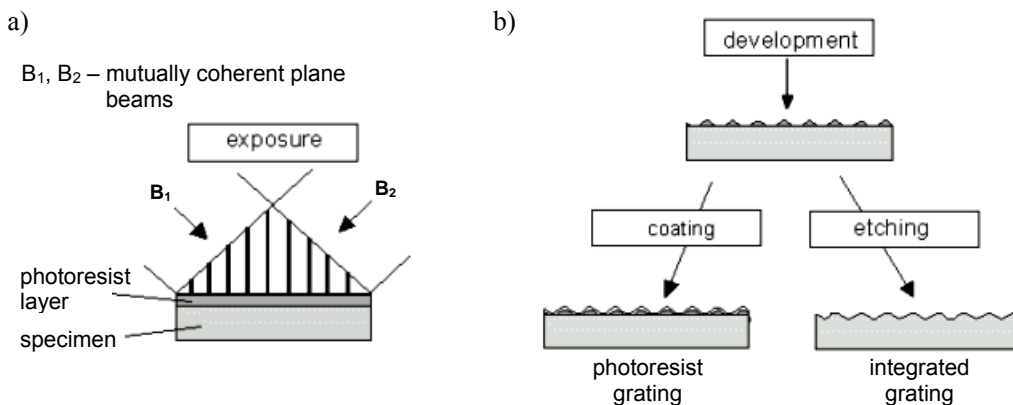


Fig. 7. The stages of producing “zero” thickness specimen grating: a) registration, b) development and final production.

8. Calibration procedure

Prior to the measurement, the following parameters should be known and/or determined and properly set:

- the period of the specimen grating,
- the quality of illuminating wavefronts and imaging optics,
- the quality of the specimen grating,
- the magnification of the imaging optics.

In the case of commercial gratings used for replication at the specimen, the producer guarantees and gives information about the grating period and its quality, which should be not worse than 1/20fringe for a 60mmx60mm photographic plate. If the specimen grating is produced in photoresist directly at the specimen, the spatial frequency and quality of the illuminating interference field is checked by comparing (i.e. observation of “moire fringes”) with the reference commercial grating whose spatial frequency is the same as the produced grating. If no fringes appear in the required field of view the periods of both gratings are equal.

The quality of the illuminating wavefronts and imaging optics should be assured by the producer, however in the case of laboratory set-ups, or after any changes in the commercial system, this parameter should be checked. It is easy to do with the help of reference (master) grating. The grating should be placed in the plane of the specimen, and after illuminating by the beams we should get so called “null fringe field” i.e. there should be no interferometric fringes at the output of the system. If more than one fringe appears the optical system of the interferometer should be corrected by the producer.

The same procedure is applied to see if the specimen grating (i.e. the reference grating after its attachment to the specimen) does not contain any distortions after the replication process. If more than one fringe appears, the process of grating replication should be repeated.

In general, the set-up in its initial state - i.e. the nonloaded specimen grating illuminated by plane beams - should not produce interferometric fringes in the measurement field of view. If there are fringes, they may be caused by:

- relative tilt between the +1 and -1 order beams diffracted at the specimen grating. In this case linear fringes are obtained and they may be removed by changing directions of the illuminating beams e.g. by proper tilt of the mirrors in the interferometric head ,
- errors in the specimen grating due to its bad quality, or
- influence of the non-planar illuminating wavefronts.

If just a single fringe appears, the initial (so called “zero”) interferogram is captured and the initial displacement field is calculated ($u_i(x,y)$ or $v_i(x,y)$) and stored in computer memory. During measurements these values are subtracted from the actual result and in this way errors of this type are eliminated.

The calibration of the optical magnification is done by taking an image of an object of known dimension in the front focal plane of the camera and associating the pixels on the camera to appropriate points on the object. The magnifications in x and y directions are calculated as:

$$\beta_x = \frac{\Delta x \cdot k_x}{d_x} \quad \text{and} \quad \beta_y = \frac{\Delta y \cdot k_y}{d_y} \quad (6)$$



where: k_x, k_y – are the actual number of pixels for the object dimensions d_x and d_y in the x and y directions.

The global verification of these settings can be achieved experimentally by a calibration specimen of known geometry such as a beam subjected to four-point bending, a disc subject to compression across the diameter, or a tensile strip. The exact circumstances of the component test must be reproduced including its geometry, material constants, temperature and loading conditions.

9. Recording and measurement procedures

The measurement procedure for grating interferometry consists of the following steps:

1. Preparation of the sample by introducing a specimen grating at its surface
2. Attachment of the sample to the load unit
3. Alignment of the measurement head towards the sample. The imaging system should be perpendicular to the surface of the sample with the grating.
4. The target area on the sample within the grating area should be chosen. The sample should be placed in the front focal plane of the imaging optics.
5. Ensure that no unforeseen relative movement of the measuring head with respect to the sample occurs. Avoid vibrations especially in the case of arrangements different from Czarnek's configuration.
6. Determine the magnification of the imaging system.
7. Identify the area of interest
8. Adjust the intensity of laser light illumination for both directions; no saturation on the CCD should occur and the full dynamic range of the camera should be used.
9. Check for good contrast of the interferometric fringes in both directions. The contrast may be often improved by adjusting the direction of polarization of the interfering beams.
10. Capture the initial set of interferograms and calculate the initial displacement fields, when the sample is under no load or under initial load.
11. Run the series of measurements. Ensure that the fringe density is not too high i.e. that they are all time-resolved by the CCD camera.
12. Evaluate the results and correct them by subtracting the initial displacement maps.
13. Calculate strain using the proper magnification and the selected length of differentiation.

10. Data processing procedures

10.1 Phase analysis

- In grating interferometry, displacement information is encoded in the intensity distribution given by an interferogram (Eq. 7). The phase of the cosinusoidal fringes in an interferogram is directly related to the displacement value i.e.

$$\phi(x, y) = \frac{4\pi}{p} u(x, y) \quad (7)$$

To numerically decode displacement maps from an interferogram, the image has to be captured by a CCD (CMOS) camera and stored in a computer. Later its digital representation is processed in



order to calculate in-plane displacement and strain maps. In principle it can be realised by so-called intensity based methods⁷ in which the locations of fringe extrema in an interferogram are digitally determined and tracked, followed by semi-automatic fringe numbering and their conversion into displacement values (given at the fringe extrema locations only). However, to provide automatic data analysis, it is advisable to use phase methods for interferogram analysis^{5,7,8}. The phase methods most widely applied for grating interferometry are:

- **temporal** phase-shifting method, TPS, in which at least 3 interferograms with phase shifts have to be employed. This method is used for static phenomena analysis, and capturing data under stable conditions,
- **spatial** carrier phase-shifting method, SCPS, where a single interferogram with spatial carrier fringes is required for displacement analysis. This method is usually used for the analysis of dynamic phenomena.

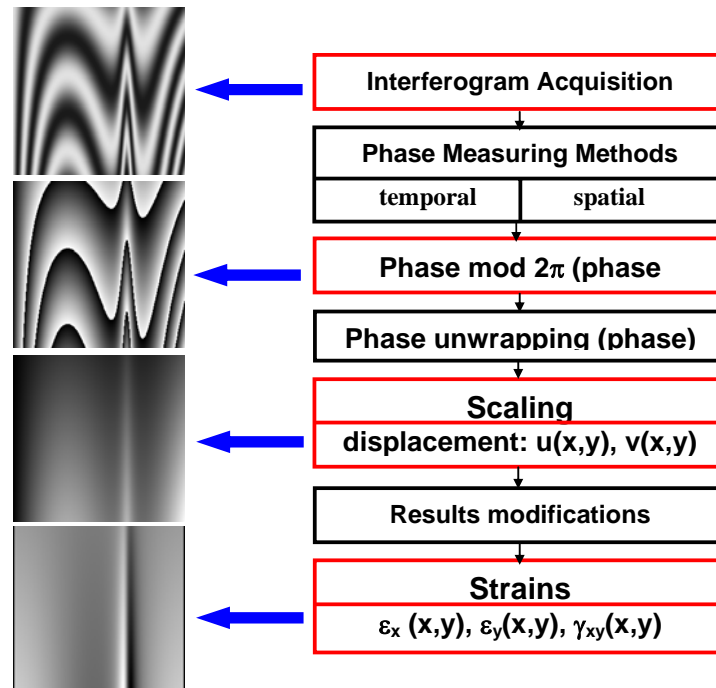


Fig. 8. The main stages of automatic, phase based, interferogram analysis.

The Fourier transform method, FT, which also requires a single interferogram for full analysis, can be also used for the analysis of dynamic phenomena. However it creates significant errors at the edges of the domain (sample discontinuity)⁷, so FT is not usually used for mechanical applications.

The main stages of interferogram(s) analysis, leading to in-plane displacement and strain maps determination, are the same for all phase methods and they are presented in Fig. 8. The details are given in the following sections.

The value directly related to displacement is the local phase of the cosinusoidal fringes in the interferogram (Eqs. 4 and 7). However this value is screened by local variations in background ($a(x,y)$) and contrast of the fringes ($b(x,y)$), therefore in order to solve this problem two approaches are implemented:



- **Temporal phase shifting method** is based on the reconstruction of the phase $\phi(x,y)$ from a number of interferograms which differ from each other by various values of a discrete phase shift φ_i . The intensity values captured $I_i(x,y)$ are:

$$I_i(x,y) = a(x,y) + b(x,y) \cdot \cos[\phi(x,y) + \varphi_i] \quad (7)$$

where $\varphi_i = (i-1)\varphi_0$ $i=1\dots M$, $M \geq 3$, $\varphi_0 = 2\pi/M$

In general only three intensity measurements are required to calculate phase from Eq. 7. However this solution requires very accurate calibration of the phase-shifter device to ensure a defined amount of phase shift, and capturing intensity data without any nonlinearity (caused often by CCD camera). This difficulty may be overcome by increasing the number of frames, and by applying a so-called $(M+1)$ algorithm⁸ it is possible to reduce this error. The most popular algorithm is the five-intensity self-calibrating algorithm with $\varphi_0 = \pi/2$. It minimizes the influence of linear errors in phase shifting and the second-order nonlinearity of the captured image intensities. In this case the phase is calculated according to the equation:

$$\varphi'(x,y) = \arctan \frac{2(I_2(x,y) - I_4(x,y))}{2I_3(x,y) - I_5(x,y) - I_1(x,y)} \quad (8)$$

The TPS method requires stable conditions during the time of capture of the set of interferograms needed for the calculations. For this reason TPS is suitable for the investigation of static events and other studies with stable conditions (i.e. no vibrations and no significant environmental condition changes).

- **Spatial carrier phase shifting method** is based on the reconstruction of the phase $\phi(x,y)$ from a single fringe pattern with linear carrier fringes⁹. The intensity captured is described by

$$I(x,y) = a(x,y) + b(x,y) \cos[\phi(x,y) + 2\pi f_{ox}x \text{ (or } 2\pi f_{oy}y)] \quad (9)$$

where f_{ox} and f_{oy} are the spatial frequencies of the linear carrier fringes added in the x or y direction to the interferogram by tilting of a mirror in the measurement set-up.

SCPS method is based on similar concept to TPS. However the phase at a given point is calculated from the intensities of neighbour points. In SCPS, a proper relation between the sampling frequency of the detector ($f_d = 1/K$, where K is the number of sampling points) and the frequency of the spatial carrier fringes f_{ox} (f_{oy}), has to be achieved in order to provide the chosen phase shift δ_i between sampling points. For similar reasons as in TPS the most popular algorithm for calculation of the phase mod 2π is the 5-point algorithm with a $\pi/2$ phase shift between the pixels. The SCPS method is widely used for automatic analysis of interferograms captured during dynamic processes investigation and when the measurements are performed in unstable conditions.

10.2 Phase unwrapping and scaling

The unwrapping or demodulation of the wrapped phase creates a continuous phase field

$$\varphi(x,y) = \varphi'(x,y) + N(x,y) \cdot 2\pi \quad (10)$$

where $N(x,y)$ is the actual integer number of the fringe.



Unwrapping algorithms are necessary to remove phase jumps from the fringe distributions. Depending on the quality and the domain discontinuities of the phase mod 2π maps, several algorithms are available^{7,10} and may alternatively be applied, including:

- line-by-line scanning (for x and y direction) which is used when the quality of the fringes is very high. It fails when noise and domain discontinuities exist,
- spanning tree algorithms which check the phase difference between a central pixel and its neighbours and chooses the route with the minimum gradient. An alternative approach uses the amplitude of each pixel as a criterion to walk through the phase map (maximum cross amplitude spanning tree). This is the most popular algorithm for maps of standard quality due to both its speed and the quality of the results.
- modulation queuing algorithm which utilises a so-called “quality map” which is defined by local modulation and phase mod 2π gradient values. This algorithm is used for noisy patterns and interferogram domains with masking,
- temporal unwrapping which utilizes consecutive phase mod 2π maps to determine actual $N(x,y)$.

After calculating the continuous phase map with proper values and sign, it is transformed to in-plane displacement maps according to the relations:

$$u(x, y) = \frac{p\phi_x(x, y)}{4\pi} \quad \text{and} \quad v(x, y) = \frac{p\phi_y(x, y)}{4\pi} \quad (11)$$

10.3 Strain calculation

If the displacement fields ($u(x,y)$, $v(x,y)$) are known it is possible to calculate the strain field for the specimen under load. In practice it is realised by differentiation of the displacement data. The in-plane strains are given by the equations:

$$\varepsilon_x = \frac{\partial u}{\partial x} = \frac{u_{i+n} - u_{i-n}}{2n\Delta x'} \quad (12a)$$

$$\varepsilon_y = \frac{\partial v}{\partial y} = \frac{v_{i+n} - v_{i-n}}{2n\Delta y'} \quad (12b)$$

$$\gamma_{xy} = \frac{\partial u}{\partial y} + \frac{\partial v}{\partial x} = \frac{u_{i+n} - u_{i-n}}{2n\Delta y'} + \frac{v_{i+n} - v_{i-n}}{2n\Delta x'} \quad (12c)$$

where: $\Delta x' = (1/\beta)\Delta x$ and $\Delta y' = (1/\beta)\Delta y$,

β - imaging system magnification,

Δx , Δy - distance between neighbouring pixels at CCD matrix plane,

$2n$ - number of pixels over which differentiation is performed.

10.3 Additional digital data processing

The digital nature of the data used in sequential stages of fringe processing makes it possible to modify the data, enhance its quality and calculate related physical quantities. The possible data processing operations include, but are not restricted to:

-*Reference Displacement Field Subtraction*. The displacement map obtained for a given loading condition contains information about the displacement under investigation and also about the total systematic error, which may include: specimen grating imperfections, optical system aberrations, initial tilt of the mirrors etc. In digital GI this systematic error may be easily removed by using



a reference map (Section 8). When the reference map is subtracted from the actual displacement map, the final map only includes information about the real displacement of the sample.

-Filtration. Very often an interferogram and/or phase map is subjected to severe high frequency noise which degrades the quality of the final displacement and strain maps. For this reason the data (at various stages of processing) are filtered with a low pass filter which removes the noise. However such filters have to be applied with great care as they can also modify the results significantly.

Masking. One of the steps in the reconstruction process is to mask those areas which do not belong to the interferogram domain. The mask is also implemented in areas where the fringe contrast is low, or the level of noise is too high.

Arithmetic Operations. Various calculations on an image or group of images (intensities and phases) can be performed. The most popular operations on images and phase maps are: sum, subtraction, difference, multiplication, calculation of RMS, minimum and maximum value etc.

10.5 Accuracy and sensitivity

Accurate results can be obtained by using accurate specimen gratings, when the following elements are extremely important:

- uniformity of the pitch “ p ” throughout the grid,
- absolute accuracy of the pitch,
- flatness of the surface of the specimen under test,
- aberrations of the illuminating beam wave front,
- good optical conjugation between the specimen grating surface and detector plane,
- error of phase calculation method and scaling.

The accuracy expected from grating interferometry measurements is between fringe/10 to fringe/40.

The sensitivity in turn is also affected by:

- the basic sensitivity, dependent on pitch “ p ” (in principle the basic sensitivity is equal to half of the pitch per fringe),
- the sensitivity of fringe analysis methods which, for the phase methods of interferogram analysis, is estimated between 1/200-1/1000fringe.

11. Areas of applications

The grating interferometry method has excellent characteristics, including: real-time whole field mapping, submicron sensitivity, high interference contrast, wide strain range, and easy alignment and operation. The results in the form of digital files can be easily adapted to test or support FEM analysis.

Grating interferometry is applied for solving various problems in experimental mechanics and material engineering. For example, it is ideally suited to the investigation of composite and smart materials in both the macro- and micro-mechanics domains, studies of joints of various types, analysis of residual stresses, investigation of fracture mechanics phenomena, local and global material constants, determination and the verification of engineering designs. It is also excellent for long time monitoring of engineering structures and the investigation of fatigue behaviour of materials and elements. Recently, numerous applications have been developed for nanomaterials studies, MEMS, MOEMS and electronic packages testing.



12. Bibliography

1. Kobayashi, A.S., ed., “*Handbook of Experimental Mechanics*”, Prentice Hall, Inc., 1987.
2. Post, D., Han, B., Ifju, P., *High Sensitivity Moiré Interferometry*, Springer-Verlag, Berlin, 1994.
3. Durelli, A.J., Parks, V.J., “*Moiré analysis of strain measurements*” Prentice-Hall, Inc., Engle Wood Cliffs, 1970.
4. *Standard Guide on Geometric Moiré for In-plane Displacement/strain Analysis*, IMiF PW, Warsaw 2003.
5. Patorski, K. “*The handbook of the moiré technique*”, Elsevier, Oxford, 1993.
6. McKelvie, J. and Patorski, K., “Influence of the slopes of the specimen grating surface on out-of-plane displacements by moiré interferometry”, *Appl. Opt.*, 27, 4603-4605, 1988.
7. Robinson, D.W., Reid, G.T., “*Fringe Pattern Measurement Techniques*”, IOP Publishing Ltd., 1993.
8. Huntley J.M., “Automated fringe pattern analysis in experimental mechanics: a review”, *Journal of Strain Analysis*, 33, 105-125, 1998.
9. Kujawinska, M. and Wójciak, J., “Spatial-carrier phase-shifting technique of fringe pattern analysis”, *Proc. SPIE*, 1508, 61-67, 1991.
10. Kujawinska, M., “Automated in-plane moiré techniques and grating interferometry” *Optical Methods in Experimental Solid Mechanics*, Springer Wien New York, 123-196, 2000.
11. Czarnek, R., “High-sensitivity moiré interferometer with compact achromatic head”, *Opt. Lasers Eng.* 13, 91-101, 1990.

